Fabrication error analysis and experimental demonstration for computer-generated holograms

Ping Zhou and James H. Burge

Aspheric optical surfaces are often tested using computer-generated holograms (CGHs). For precise measurement, the wavefront errors caused by the CGH must be known and characterized. A parametric model relating the wavefront errors to the CGH fabrication errors is introduced. Methods are discussed for measuring the fabrication errors in the CGH substrate, duty cycle, etching depth, and effect of surface roughness. An example analysis of the wavefront errors from fabrication nonuniformities for a phase CGH is given. The calibration of these effects for a CGH null corrector is demonstrated to cause measurement error less than 1 nm.

OCIS codes: 050.1380, 090.2880, 120.2880.

1. Introduction

Optical elements with large aspheric departures are often tested with the help of computer-generated holograms (CGHs).[1–3] The primary role of CGHs is to generate reference wavefronts of any desired shape. An accurately drawn pattern on the CGH provides accurate wavefront control. The precision of the CGH pattern affects the accuracy and validity of the measurement results. The CGH errors can be design errors, alignment errors, or fabrication errors. The surface measurement can suffer from all these errors. The CGH design errors and alignment errors are discussed elsewhere.[4,5] In this paper, we only focus on how the CGH fabrication errors affect the wavefront performance.

The CGH fabrication errors can be classified into five types:

- Substrate figure errors: substrate surface variation from its ideal shape.
- Pattern distortion errors: displacement of the recorded pattern from its ideal position.
- Duty-cycle errors: variation in duty cycle.
- Etching depth errors: variation in etching depth.
- Surface roughness errors: variation in surface roughness.

The authors are with the College of Optical Sciences, University of Arizona, Tucson, Arizona 85721, USA. P. Zhou's e-mail address is pzhou@optics.arizona.edu.

Received 28 July 2006; accepted 19 September 2006; posted 5 October 2006 (Doc. ID 73546); published 25 January 2007.

0003-6935/07/050657-07$15.00/0

The effects of all these fabrication errors are coupled together, and it is difficult to decouple the individual effects of each error source on the wavefront. Chang and Burge[6,7] first developed a parametric model to relate the fabrication errors to the wavefront performance. This model is summarized and extended in this paper. This parametric model can help estimate wavefront measurement errors due to a CGH in optical testing. Some methods to determine the fabrication nonuniformities in the duty cycle, etching depth, and surface roughness are provided in Section 3. A wavefront error analysis for a phase CGH is shown in Section 4. The calibration of the CGH substrate is demonstrated in Section 5 to provide a measurement accurate to about 1 nm rms.

2. Parametric Model

The binary, linear grating model is used to build the parametric model based on scalar diffraction theory. The scalar theory assumes that the wavelength of the incident light is much smaller than the grating period S. Only the far-field diffraction effects will be of interest. Furthermore, it is assumed that the grating is illuminated with a planar wavefront at normal incidence. Figure 1 illustrates a binary, linear grating.

The grating is defined by the period S and the etching depth t. Duty cycle is defined as $D = b/S$, where b is width of the etched area. A_0 and A_1 correspond to the amplitudes of the output wavefront from the unetched and etched areas of the grating, respectively. The phase function ϕ represents the phase difference between rays from the peaks and rays from the valleys of the grating structure, which equals $2\pi(n - 1)t/\lambda$ for the grating in transmission mode.

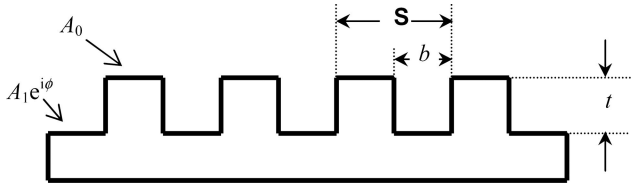

Fig. 1. Binary, linear grating profile.

The approach of the linear grating model for CGH characterization has already been developed by Chang and Burge.[6,7] The diffracted wavefront phase is Ψ. The wavefront phase sensitivity functions $\partial\Psi/\partial D$ and $\partial\Psi/\partial\phi$ are introduced to specify the wavefront error caused by small deviations in duty cycle ΔD and in phase function $\Delta\phi$. Here, the model is extended with the introduction of the wavefront sensitivity function $\partial\Psi/\partial(A_0/A_1)$, which describes the wavefront error caused by a small deviation of the ratio of two amplitudes, $\Delta(A_0/A_1)$.[8] The deviation of the amplitude ratio is due to local surface roughness variations. Table 1 summarizes the wavefront sensitivity functions and the diffraction efficiencies for the zero and the nonzero diffraction orders.

The sensitivity functions can be evaluated directly to give the wavefront error due to variations in duty cycle D, etch depth t, or amplitude ratio A_0/A_1. These functions are shown in Eqs. (1)–(3), respectively:

$$\Delta W_D = \frac{1}{2\pi}\frac{\partial\Psi}{\partial D}\Delta D = \frac{1}{2\pi}\frac{\partial\Psi}{\partial D}\left(\frac{\Delta D}{D}\right)D, \tag{1}$$

$$\Delta W_\phi = \frac{\partial\Psi}{\partial\phi}\Delta\phi = \frac{\partial\Psi}{\partial\phi}\left(\frac{\Delta\phi}{\phi}\right)\phi, \tag{2}$$

$$\Delta W_{A_0/A_1} = \frac{1}{2\pi}\frac{\partial\Psi}{\partial(A_0/A_1)}\Delta\left(\frac{A_0}{A_1}\right), \tag{3}$$

where ΔD is the duty-cycle variation across the grating; ΔW_D is the wavefront variation in waves due to duty-cycle variation; $\Delta\phi$ is the etching depth variation in radians across the grating, ΔW_e is the wavefront variation in waves due to etching depth variation; $\Delta(A_0/A_1)$ is the variation of the ratio of A_0 to A_1; and $\Delta W_{A_0/A_1}$ is the wavefront variation in waves due to amplitude variation.

As long as the duty cycle, etching depth, and amplitude vary over spatial scales that are large compared to the grating spacing, Eqs. (1)–(3) can be used to determine the coupling between fabrication errors and system performance. The wavefront sensitivity functions provide a means of calculating the wavefront phase changes that result from the fabrication nonuniformities. They can be used to identify which hologram structures are the most or the least sensitive to those fabrication uncertainties. The information may also be used to estimate error budgets for applications using the CGHs.

Note that the wavefront phase change caused by a constant fabrication error in duty cycle, etching depth, or amplitude ratio cannot be measured. This is because the constant phase change is regarded as a piston and it is often removed in optical testing. This parametric model relates the wavefront errors to the fabrication nonuniformities. The wavefront error can be estimated if the fabrication nonuniformities in duty cycle, etching depth, and amplitudes are known.

Another wavefront error is from CGH pattern position. Pattern position error, also called pattern distortion, means that the recorded pattern in a CGH is displaced from its ideal position. The amount of wavefront errors produced by the CGH pattern distortions can be expressed as

$$\Delta W(x, y) = -m\lambda\frac{\varepsilon}{S}, \tag{4}$$

Table 1. Summary of Equations for Parametric Model Analysis

	Zero Order ($m = 0$)	Nonzero Order ($m \pm 1, \pm 2, \ldots$)
	Diffracted Wavefront	
η, diffraction efficiency	$A_0^2(1-D)^2 + A_1^2D^2 + 2A_0A_1D(1-D)\cos(\phi)$	$[A_0^2 + A_1^2 - 2A_0A_1\cos(\phi)]D^2\,\mathrm{sinc}^2(mD)$
$\tan(\Psi)$ Ψ, wavefront phase	$\dfrac{A_1D\sin(\phi)}{A_0(1-D) + A_1D\cos(\phi)}$	$\dfrac{A_1\sin(\phi)\mathrm{sinc}(mD)}{[-A_0 + A_1\cos(\phi)]\mathrm{sinc}(mD)}$
	Sensitivity Functions	
$\dfrac{\partial\eta}{\partial D}$	$-2A_0^2(1-D) + 2A_1^2D + 2A_0A_1(1-2D)\cos\phi$	$2[A_0^2 + A_1^2 - 2A_0A_1\cos(\phi)]D\,\mathrm{sinc}(2mD)$
$\dfrac{\partial\eta}{\partial\phi}$	$-2A_0A_1D(1-D)\sin\phi$	$2A_0A_1\sin\phi\,D^2\,\mathrm{sinc}^2(mD)$
$\dfrac{\partial\Psi}{\partial D}$	$\dfrac{A_0A_1\sin\phi}{A_1^2D^2 + A_0^2(1-D)^2 + 2A_0A_1D(1-D)\cos\phi}$	$\begin{cases}\infty, & \text{for } \mathrm{sinc}(mD) = 0\\ 0, & \text{otherwise}\end{cases}$
$\dfrac{\partial\Psi}{\partial\phi}$	$\dfrac{A_1^2D^2 + A_0A_1D(1-D)\cos\phi}{A_1^2D^2 + A_0^2(1-D)^2 + 2A_0A_1D(1-D)\cos\phi}$	$\dfrac{A_1^2 - A_0A_1\cos\phi}{A_1^2 + A_0^2 - 2A_0A_1\cos\phi}$
$\dfrac{\partial\Psi}{\partial(A_0/A_1)}$	$\dfrac{-D(1-D)\sin\phi}{(A_0/A_1)^2(1-D)^2 + D^2 + 2D(1-D)(A_0/A_1)\cos\phi}$	$\dfrac{\sin\phi}{(A_0/A_1)^2 + 1 - 2(A_0/A_1)\cos\phi}$

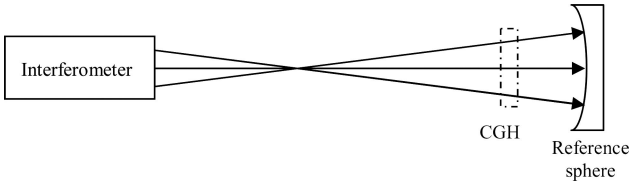

Fig. 2. Setup of CGH substrate measurement.

where ε is the grating position error in the direction perpendicular to the pattern. The produced wavefront phase errors due to pattern distortions are linearly proportional to the diffraction order number and inversely proportional to the local fringe spacing.[9] CGH pattern distortion errors do not affect the zero-order diffracted beam. Pattern distortion can be measured with a microdensitometer or by using an interferometric method.[10,11]

3. Measurement of Fabrication Errors

To quantify the wavefront error in optical testing, the fabrication nonuniformities for each error source must be determined. These fabrication nonuniformities can be obtained by measuring a set of sampled points over the CGH.

A. Substrate Measurement

Substrate errors are typically of low spatial frequencies. Their effects on the wavefront depend on the applications of the CGH. If the CGH is used in reflection, a surface defect on a CGH substrate with a peak-to-valley deviation of δs, where s refers to the ideal surface figure, will produce a wavefront error of $2\delta s$. A transmission CGH that has the same peak-to-valley surface defect, on the other hand, will produce a wavefront phase error of $(n - 1)\delta s$, where n is the index of refraction of the substrate. The substrate errors influence all the diffraction orders equally.[12]

One method of eliminating substrate errors in a CGH is to measure the flatness of the substrate before the grating patterns are written. This procedure can be done on a Fizeau interferometer. Another method is to measure the effect of surface irregularities using the zero-order diffraction from the CGH, and subtract this from the nonzero-order surface measurement. A test setup is illustrated in Fig. 2, where the CGH is placed in a diverging beam instead of a collimated beam because that is the actual working configuration for this CGH. The reference sphere is first measured, then the wavefront with the CGH is tested. The difference of these two measurements depicts the transmitted wavefront error of the CGH in zero-order diffraction, which is mainly CGH substrate error.

Note that besides the CGH substrate error, the wavefront errors introduced by the nonuniformities in duty cycle, etching depth, and amplitude ratio also affect the zero-order measurement. These errors affect zero and nonzero orders differently. When we subtract the nonzero-order surface measurement from the zero-order measurement, the CGH substrate error can be totally removed, leaving the residual wavefront errors from the fabrication nonuniformities.

B. Duty Cycle and Etching Depth Measurement

Variations in duty cycle and etching depth can be measured using either an atomic force microscope or an interference microscope, which provide the surface relief of the CGH. Another method is to measure the diffraction efficiencies of several diffraction orders and then fit the duty cycle and etching depth. A set of the sampled points should be measured to obtain the variations in duty cycle and etching depth. The duty cycle and etching depth at each sampled point are determined by using the nonlinear least-squares fit. The CGH is illuminated with a finite small laser spot, so the fitted results are the average duty cycle and etching depth over that illuminated area.

To verify the feasibility of the second method, a Monte Carlo analysis was used to find the relationship between the number of diffraction orders measured and the accuracy obtainable for the duty cycle and etching depth. The results shown in Fig. 3 are for a 1000-trial Monte Carlo simulation. The nominal duty cycle and etching depth are 0.49 and 0.33λ,

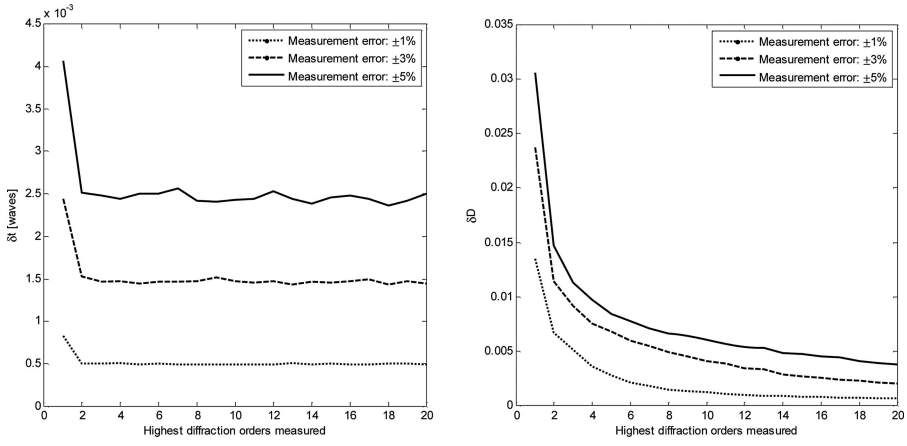

Fig. 3. Monte Carlo simulation on (left) etching depth and (right) duty cycle.

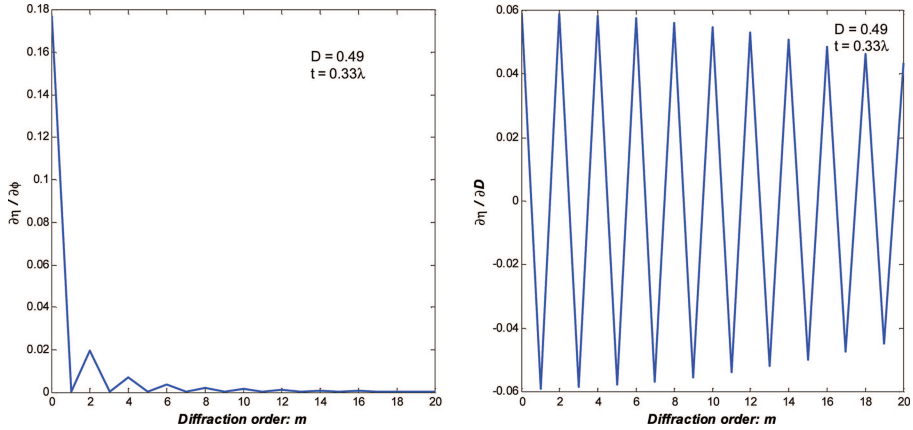

Fig. 4. (Color online) Sensitivity of diffraction efficiencies to (left) etching depth and (right) duty cycle.

respectively, in this simulation. These are the measured parameters of a CGH demonstrated in Section 4. A_0 and A_1 are assumed to be unity, since it is a phase CGH. A uniform-distributed random error is added to each diffraction efficiency measurement. Measurement errors of up to $\pm 1\%$, $\pm 3\%$, and $\pm 5\%$ for each order are assumed in the analysis. δt and δD are the standard deviations of the etching depth and duty cycle of the 1000 trials, which represent the measurement confidence level of the etching depth and duty cycle.

The simulation demonstrates that δt does not change significantly by increasing the number of measured diffraction orders. It is proportional to the measurement error. δD decreases with an increase in the number of measured diffraction orders and finally converges when the number of diffraction orders is sufficiently large. This can be explained by the sensitivity functions of the diffraction efficiencies to the etching depth and duty cycle $\partial\eta/\partial\phi$, $\partial\eta/\partial D$. Figure 4 shows the sensitivity functions for each diffraction order when the duty cycle is 0.49 and the etching depth is 0.33λ. The sensitivity of the diffraction efficiency to the etching depth drops dramatically at higher diffraction orders, while it oscillates around zero for the duty cycle. This means that the higher diffraction orders do not contribute considerably to the knowledge of the etching depth, so the Monte Carlo simulation gives us a relatively flat curve for δt. However, higher diffraction orders can increase the measurement accuracy of the duty cycle.

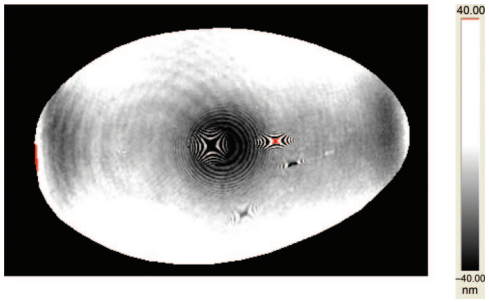

Fig. 5. (Color online) Transmitted wavefront of the CGH substrate.

By careful measurement, we can control the measurement error within $\pm 1\%$. In this case, δt and δD are about 0.0005λ and 0.0015, respectively, if we measure up to the ± 10th diffraction order. These accuracies are sufficient to evaluate the nonuniformities in the duty cycle and etching depth.

C. Amplitude Variation Measurement

The amplitude of the light from the etched regions can vary due to limitations in the reactive ion etching process. The surface roughness of the etched area may vary due to etching, so the light incident on the CGH scatters differently. By assuming that the surface roughness is much smaller than the wavelength of incident light, the coupling of the scattered light to the diffracted light can be ignored. However, the scattering will decrease the amplitude of the diffracted light. This leads to an amplitude ratio variation over the CGH. It is difficult to measure the intensities (or amplitudes) from the etched area and unetched area of the CGH directly. One useful method is to measure the surface roughness of both areas and then calculate the scattered loss. The scattered loss is zero when the surface is perfectly flat, and it increases with increasing surface roughness. A simple approximate formula to calculate the total integrated scatter (TIS) for the transmitted light is

$$I_{scat} \approx (2\pi\sigma)^2 = [2\pi(n-1)R_q/\lambda]^2, \tag{5}$$

Table 2. Duty Cycle and Etching Depth of the Five Positions

	D	t (waves)
Point 1	0.4897	0.3274
Point 2	0.4906	0.3315
Point 3	0.4897	0.3317
Point 4	0.4904	0.3326
Point 5	0.4881	0.3275
Average	0.4897	0.33014
rms variation	0.0009	0.0022
rms variation in percentage	0.18%	0.67%

Table 3. Surface Roughness Measurement

	Unetched Area		Etched Area		
	rms roughness (nm)	I_{scat}	rms roughness (nm)	I_{scat}	Ratio of amplitudes $\lvert A_0/A_1 \rvert$
Point 1	0.950	0.00002	2.188	0.00012	1.000048
Point 2	1.090	0.00003	1.540	0.00006	1.000015
Point 3	1.110	0.00003	1.840	0.00008	1.000027
Point 4	2.000	0.00010	2.663	0.00017	1.000038
Point 5	1.738	0.00007	2.169	0.00012	1.000021
			Average		1.000030
			rms variation		0.000033
			rms variation in percentage		0.000033

where σ^2 is the wavefront variance in units of waves, n is the index of refraction of the CGH substrate, and R_q is the rms surface roughness. The TIS for the reflected light is $I_{scat} = (4\pi R_q/\lambda)^2$. The surface roughness can be measured by an interference microscope. The intensity of the light from the etched and unetched regions can be determined by

$$I = 1 - I_{scat}. \tag{6}$$

The variation of the surface roughness causes different amounts of the scattered loss, which leads to the wavefront errors.

The effect of the surface roughness comes in very slowly. Assume the refractive index of the substrate is 1.5, and the wavelength of interest is 632.8 nm. The transmittance of the light at the grating interface is 96% based on the Fresnel formula. If the surface roughness of the etched area is 2 ± 0.5 nm rms, the scattered loss would be $0.01\% \pm 0.005\%$, and the amplitude variation would be 0.003%. For the above case of 49% duty cycle and 0.33λ etching depth, the wavefront errors from the surface roughness for the zero and nonzero orders would be -0.00244 and 0.00086 nm, respectively.

4. Error Analysis for a Phase Computer-Generated Hologram

The fabrication nonuniformities of a 5 in. (1 in. = 2.54 cm) phase CGH used for testing an off-axis parabola (OAP) was measured. The CGH was designed with a duty cycle of 50% and an etching depth of 0.33λ. At a 50% duty cycle, the wavefront sensitivities to the etching depth are the same for both the zero order and the first order. Once the first-order measurement is subtracted from the zero-order one, the wavefront errors from the etching depth can be canceled. An etching depth of 0.33λ is an optimized parameter that gives good diffraction efficiencies with fewer wavefront errors from the duty cycle and amplitude ratio.[13]

The CGH substrate error was measured using the zero-order diffraction of the CGH. A 4D Technology PhaseCam 4010 interferometer with an $f/7$ transmission objective was used. The test setup was similar to that shown in Fig. 2. The transmitted wavefront showed 13.6 nm rms. Figure 5 shows the measured transmitted wavefront.

The duty cycle and etching depth variations were estimated using measured diffraction efficiencies up to the 11th orders. The CGH was illuminated with a 1 mm diameter collimated HeNe laser beam. A Newport low-power 918-UV detector and a 2930-C powermeter were used to measure the power of each diffraction order. Five points on the CGH were chosen to measure the fabrication nonuniformities. For each power measurement, 500 data points with an interval time of 20 ms were averaged by the powermeter. The background light was subtracted from each measurement. A nonlinear least-squares fit was applied to find the duty cycles and etching depths of these five positions, shown in Table 2. The rms variations of the duty cycle and the etching depth were determined to vary by 0.18% and 0.67%.

The surface roughness of the etched area and unetched area were tested on a WYKO NT-2000 microscope. Table 3 shows that the amplitude variation due to scattering is 0.0033% rms, which is small enough to be neglected.

The first-order wavefront of the CGH is used to test the OAP. Table 4 lists all the wavefront errors from the CGH. The estimated root-sum-square (rss) wavefront error of the first-order measurement is 13.6 nm. Duty-cycle nonuniformities have no effect on the wavefront error for the first-order diffraction. Among all the fabrication errors, the substrate error is dominant. To achieve higher measurement accuracy, the substrate errors need to be calibrated.

Table 4. Wavefront Errors from CGH Fabrication Nonuniformities without Substrate Calibration

Source of Errors	Description	Measured Variation	Sensitivities	rms Wavefront Errors at First Order (nm)
CGH substrate	Transmitted wavefront error	13.6 nm	1:1	13.6
Etching depth	Effect on diffracted wavefront	0.67%	$\frac{\delta\Psi_{m=1}}{\delta\phi}$	0.700
Duty cycle	Effect on diffracted wavefront	0.18%	0	0
Amplitude ratio	Effect on diffracted wavefront	0.0033%	$\frac{\delta\Psi_{m=1}}{\delta(A_0/A_1)}$	0.001
Root-sum-square error				13.6

Table 5. Wavefront Errors from CGH Fabrication Errors after Subtracting the Zeroth-Order Measurement

Source of Errors	Measured Variation	Sensitivities	rms Wavefront Errors (nm)
Etching depth error	0.67%	$\frac{\partial \Psi_{m=1}}{\partial \phi} - \frac{\partial \Psi_{m=0}}{\partial \phi}$	0.056
Duty-cycle error	0.18%	$-\frac{\partial \Psi_{m=0}}{\partial D}$	0.300
Amplitudes error	0.0033%	$\frac{\partial \Psi_{m=1}}{\partial (A_0/A_1)} - \frac{\partial \Psi_{m=0}}{\partial (A_0/A_1)}$	0.004
Root-sum-square error			0.3

The CGH substrate errors can be removed by subtracting the zero-order measurement from the OAP wavefront measurement. However, the wavefront errors caused by the fabrication nonuniformities cannot be totally removed. With the fabrication errors we measured above, we assessed both the zero-order and the first-order diffraction wavefronts, and then subtracted one from the other for each error source. Table 5 lists the residual wavefront errors for each error source. The rss wavefront error drops from 13.6 to 0.3 nm.

Note that the pattern distortion error is not included in the analysis in Table 5 because we did not measure the pattern distortion. Assuming the pattern distortion error is 0.1 μm for the 20 μm spacing and the wavelength of interest is 632.8 nm, then the wavefront error caused by pattern distortion for the first order is 3.2 nm. The pattern distortion becomes the most important error after calibrating the CGH substrate error.

The error analysis of this phase CGH demonstrates that the CGH substrate is the primary error source. The wavefront errors caused by the etching depth, duty cycle, and amplitude are determined to be small enough that we cannot measure them using the interferometer. These errors can be neglected in optical testing.

5. Demonstration of Substrate Calibration

To demonstrate that the substrate error can be calibrated by the zero-order wavefront, a custom CGH with 30% duty cycle and 0.35λ etching depth was fabricated, where the wavelength of interest is 632.8 nm. The CGH has a diameter of 15 mm and generates a spherical wavefront. A reference sphere is used to reflect the light back for both the zero-order and first-order measurements. Figure 6 illustrates the setup of the experiment. The first-order phase map was subtracted from the zero-order one to remove the CGH substrate error. The difference of these two phase maps should record only the fabrication errors in duty cycle, etching depth, amplitude ratio, and pattern distortion. The reference sphere does not introduce any errors in the measurement because it cancels out during the subtraction.

Table 6. Substrate Calibration

	rms Error: Zero Order (nm)	rms Error: First Order (nm)	Measured Difference (nm)
Configuration 1	1.677	1.648	0.714
Configuration 2	7.596	7.801	0.779
Configuration 3	16.82	17.43	1.291

To increase the CGH substrate error, a glass window was placed between the interferometer and the CGH, which is equivalent to the CGH substrate error. Table 6 shows measurement results of three configurations with different amounts of the equivalent substrate errors. Configuration 1 has no glass window in the setup, while configurations 2 and 3 have different window glasses. Up to about 15 nm substrate error is introduced in configuration 3. Tilt, power, and astigmatism from the optical test are removed in the measurement, which come from system alignment. For all cases, the difference of the first-order and zero-order wavefront is about 1 nm rms. The wavefront errors from both fabrication nonuniformities and measurement noises contribute to this difference. This experiment shows that the substrate errors can be removed by subtracting the first-order wavefront from the zero-order one.

6. Conclusions

This paper has introduced the parametric model that relates the wavefront performance to the fabrication errors of CGHs and has discussed the methods for determining these fabrication errors. An example of the error analysis for a phase CGH was given by

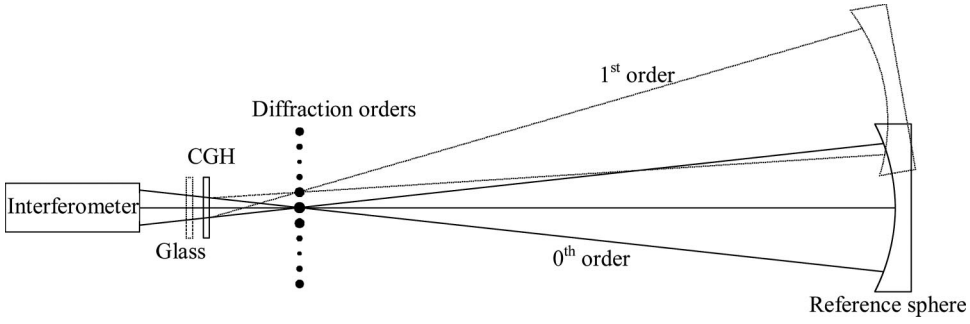

Fig. 6. Setup of the CGH substrate calibration.

applying this parametric model. This example shows that the substrate error is the dominant error from the CGH and that it can be removed by subtracting the first-order measurement from the zero-order one. After performing the substrate calibration, the wavefront errors from the fabrication nonuniformities in duty cycle, etching depth, and amplitude ratio are not significant. This method was applied to an experiment in which several cases of substrate errors were analyzed, where the rms error is reduced from 17 to 1 nm in the worst case.

The authors thank Steven M. Arnold from Diffraction International for fabrication of the CGH and Proteep C. V. Mallik for his help on the experiments.

References and Notes

1. D. Malacara, *Optical Shop Testing,* 2nd ed. (Wiley, 1992).
2. S. M. Arnold, "How to test an asphere with a computer generated hologram," in *Holographic Optics,* Proc. SPIE **1052,** 191–197 (1989).
3. H. J. Tiziani, S. Reichelt, C. Pruss, M. Rocktaeschel, and U. Hofbauer, "Testing of aspheric surfaces," in *Lithographic and Micromachining Techniques for Optical Component Fabrication,* Proc. SPIE **4440,** 109–119 (2001).
4. R. Schreiner, T. Herrmann, J. Röder, S. Müller-Pfeiffer, and O. Falkenstörfer, "Design considerations for computer generated holograms as supplement to Fizeau interferometers," in *Optical Fabrication, Testing, and Methodology II,* Proc. SPIE **5965,** 59650K (2005).
5. E. Curatu and M. Wang, "Tolerancing and testing of CGH aspheric nulls," in *Optical Manufacturing and Testing III,* Proc. SPIE **3782,** 581–599 (1999).
6. Y. C. Chang and J. H. Burge, "Errors analysis for CGH optical testing," in *Optical Manufacturing and Testing III,* Proc. SPIE **3782,** 358–366 (1999).
7. Y. C. Chang, P. Zhou, and J. H. Burge, "Analysis of phase sensitivity for binary computer generated holograms," Appl. Opt. **45,** 4223–4234 (2006).
8. P. Zhou and J. H. Burge are preparing a paper to be called "Coupling of surface roughness on the wavefront performance for diffraction grating."
9. A. F. Fercher, "Computer-generated holograms for testing optical elements: error analysis and error compensation," Opt. Acta **23,** 347–365 (1976).
10. J. C. Wyant, P. K. O'Neill, and A. J. MacGovern, "Interferometric method of measuring plotter distortion," Appl. Opt. **13,** 1549–1551 (1974).
11. A. Ono and J. C. Wyant, "Plotting errors measurement of CGH using an improved interferometric method," Appl. Opt. **23,** 3905–3910 (1984).
12. J. Burge, "A null test for null correctors: error analysis," in *Quality and Reliability for Optical Systems,* Proc. SPIE **1993,** 86–97 (1993).
13. P. Zhou and J. H. Burge are preparing a paper to be called "Optimization design of computer generated holograms to improve the performance."